

Superconductivity in Sr₂RuO₄-Sr₃Ru₂O₇ eutectic crystals

R. Fittipaldi^{1,2}, A. Vecchione^{1,2}, R. Ciancio^{1,2,5}, S. Pace^{1,2}, M. Cuoco^{1,2}, D. Stornaiuolo³,
D. Born³, F. Tafuri^{3,4}, E. Olsson⁵, S. Kittaka⁶, H. Yaguchi⁶, and Y. Maeno⁶

¹ *Laboratorio Regionale SuperMat, CNR-INFN Salerno, Baronissi (Sa), Italy*

² *Dipartimento di Fisica "E.R. Caianiello", Università di Salerno, Baronissi(Sa),Italy*

³ *CNR-INFN Coherentia and Dipartimento di Scienze Fisiche , Università di Napoli Federico II, Napoli, Italy*

⁴ *Dipartimento Ingegneria dell'Informazione, Seconda Università di Napoli, Aversa (CE), Italy*

⁵ *Department of Applied Physics, Chalmers University of Technology, University of Chalmers, Goteborg and*

⁶ *Department of Physics, Kyoto University, Kyoto 606-8502, Japan*

Superconducting behavior has been observed in the Sr₂RuO₄-Sr₃Ru₂O₇ eutectic system as grown by the flux-feeding floating zone technique. A supercurrent flows across a single interface between Sr₂RuO₄ and Sr₃Ru₂O₇ areas at distances that are far beyond those expected in a conventional proximity scenario. The current-voltage characteristics within the Sr₃Ru₂O₇ macrodomain, as extracted from the eutectic, exhibit signatures of superconductivity in the bilayered ruthenate. Detailed microstructural, morphological and compositional analyses address issues on the concentration and the size of Sr₂RuO₄ inclusions within the Sr₃Ru₂O₇ matrix. We speculate on the possibility of inhomogeneous superconductivity in the *eutectic* Sr₃Ru₂O₇ and exotic pairing induced by the Sr₂RuO₄ inclusions.

Layered strontium ruthenates are currently a subject of intense investigation due to many fascinating properties exhibited by Sr₂RuO₄ in the context of unconventional superconductivity and by Sr₃Ru₂O₇ in relation with metamagnetic quantum criticality[1, 2, 3, 4, 5]. The recent progress[6] in preparing samples with eutectic solidification of superconducting(SC) Sr₂RuO₄ and metamagnetic Sr₃Ru₂O₇ have opened a novel route to explore systems where unconventional superconductivity and collective magnetic behavior can be matched at the nanoscale with high interface quality. A preliminary characterization of this type of compound, via current-voltage (*I-V*) measurements, has shown an unusual temperature and field behavior of the critical current[7]. It emerged a picture of a strongly coupled Josephson weak-link network where the Sr₂RuO₄ grains should be responsible for the SC behavior mediated by an unusual proximity effect through the Sr₃Ru₂O₇ domains. The screening fraction has been estimated via susceptibility measurements to be nearly 100% of the volume of Sr₃Ru₂O₇ region[8]. The peculiar sensitivity of the screening to small applied fields has been considered as an evidence of an intrinsic granularity. So far, the nature of the SC state in the eutectic turns out to be controversial, mainly for the lack of detailed structural characterization about the concentration and the size of Sr₂RuO₄ inclusions within Sr₃Ru₂O₇ eutectic domain.

In this letter, we perform a detailed transport and structural analysis of the Sr₂RuO₄-Sr₃Ru₂O₇ compound profiting of a special sample selection within the eutectic itself. We have investigated: i) one nominal Sr₂RuO₄-Sr₃Ru₂O₇ interface and ii) a macrodomain of Sr₃Ru₂O₇. The *I-V* characteristics measured in i) shows a supercurrent I_c even at distances of $\sim 2000 \mu\text{m}$ far from the interface between Sr₂RuO₄ and Sr₃Ru₂O₇. I_c does not decay exponentially as in a conventional proximity ef-

fect. The same measurements performed for the case ii) give evidence of a supercurrent flowing through the Sr₃Ru₂O₇ domain as well. Systematic compositional and microstructural studies yield limits on the distribution and size of Sr₂RuO₄ inclusions within the Sr₃Ru₂O₇ matrix. Their presence cannot be more than a few percent of the total volume and they consist of one, two or three individual layers of Sr₂RuO₄ in a Sr₃Ru₂O₇ matrix interrupting the stack of the bilayered structure along the *c*-axis. We speculate that the small amount of Sr₂RuO₄ within the Sr₃Ru₂O₇ cannot account for the observed superflow at the interface and within the Sr₃Ru₂O₇ even as a percolative phenomena.

The synthesis of Sr₂RuO₄-Sr₃Ru₂O₇ eutectic crystals by a flux-feeding floating zone technique has been previously reported[6]. Inspection with the polarized light optical microscope (PLOM) within the *a-c* planes confirmed the expected lamellar solidification microstructure of the eutectic Sr₂RuO₄-Sr₃Ru₂O₇[6]. The morphology of the crystals has been investigated by scanning electron microscope (SEM) equipped with electron back scattered (EBS) detector, yielding no detectable precipitates. Moreover, likewise to other single-phase ruthenates, the eutectic crystals can be cleaved in the *a-b* planes. The crystal selected for this work (hereafter called sample 1) is basically composed both of lamellar pattern and of large domains of the two phases. From this sample, we have cut a piece (sample 2) composed by two macrodomains of Sr₂RuO₄ and Sr₃Ru₂O₇ in contact with each other. This is a crucial aspect for the present investigation: the requirement is to obtain a controlled arrangement of the two phases inside the sample. Indeed, to make sure that just one interface is involved in the transport measurements, both the top and bottom sides of the *a-c* surface have been polished until the same pattern of Sr₂RuO₄ and Sr₃Ru₂O₇ regions is achieved. The final

dimensions of the sample 2 were $5.61 \times 0.32 \times 0.66 \text{ mm}^3$. The composition of the sample 2 has been carried out both by energy dispersive spectroscopy (EDS) and by wavelength dispersive spectroscopy (WDS). EDS analysis performed over different areas gave evidence of the presence, within the sample, of only two distinct phases identified as Sr_2RuO_4 and $\text{Sr}_3\text{Ru}_2\text{O}_7$. The constant value $n=2 N(\text{Ru})/N(\text{Sr})$ as obtained by WDS analysis ($N(\text{Ru})$ and $N(\text{Sr})$ being the number of moles for Sr and Ru, respectively), demonstrated the homogeneity of the two phases within the bulk region. Spatially resolved WDS presented no signs of gradient concentration of $\text{Sr}_3\text{Ru}_2\text{O}_7$ or Sr_2RuO_4 approaching the interface. Scans of approximately 10 hours has been carried out in the wavelengths range $0.248 - 2.379 \text{ nm}$ on different regions of the sample to check the presence of spurious elements with Z ranging from 5(B) and 83(Bi). All the observed peaks have been attributed to X-rays characteristic of Sr or Ru. No magnetically active element has been found. The analysis on the Sr_2RuO_4 and $\text{Sr}_3\text{Ru}_2\text{O}_7$ domains did not reveal spurious elements within the sensitivity of the experiment. Subsequently, from sample 2 we selected a piece of dimensions $2.82 \times 0.32 \times 0.66 \text{ mm}^3$ nominally consisting only of $\text{Sr}_3\text{Ru}_2\text{O}_7$ phase (sample 3). This sample showed few isolated Sr_2RuO_4 clusters on the surface of $\sim 10 \mu\text{m}^2$ with an average distance among them of $\sim 30 \mu\text{m}$. The amount of Sr_2RuO_4 clusters visible in SEM on the surface of sample 3 has been evaluated to be about 0.5% of the $\text{Sr}_3\text{Ru}_2\text{O}_7$ domain.

To detect the presence of Sr_2RuO_4 nanodomains finely dispersed within the $\text{Sr}_3\text{Ru}_2\text{O}_7$ layers at atomic level, we have performed a microstructural analysis by means of transmission electron microscope(TEM) through different areas of the sample 3. A representative TEM image of different areas of sample 3 away from Sr_2RuO_4 clusters is reported in Fig. 1. It is possible to notice that the $\text{Sr}_3\text{Ru}_2\text{O}_7$ domain, as extracted from the eutectic, is homogeneous and free of defects over areas of several nanometers. A detailed inspection reveals the presence of one or two unit cells corresponding to the Sr_2RuO_4 structure, occurring as stacking faults monolayers that, along the c -axis, interrupt the $\text{Sr}_3\text{Ru}_2\text{O}_7$ periodicity. The systematic scan of a large area within sample 3 indicates that such type of stacking faults defects are of nanometric size and their amount can be estimated to be not greater than a few percent of the total area analyzed.

As a confirmation of such dispersion of non stoichiometric defects with respect to the $\text{Sr}_3\text{Ru}_2\text{O}_7$ structure, we traced a grid of 20×20 points on the sample 3 to perform EDS measurements by avoiding the few regions where the clusters of Sr_2RuO_4 are observable. The value obtained for the Sr/Ru ratio is $n = 1.304 \pm 0.012$, that turns out to be very close to the expected one for an ideal $\text{Sr}_3\text{Ru}_2\text{O}_7$ crystal ($n=1.333$). The deviation from the ideal value in the direction of the monolayer stoichiometry can be read as a consequence of Sr_2RuO_4 de-

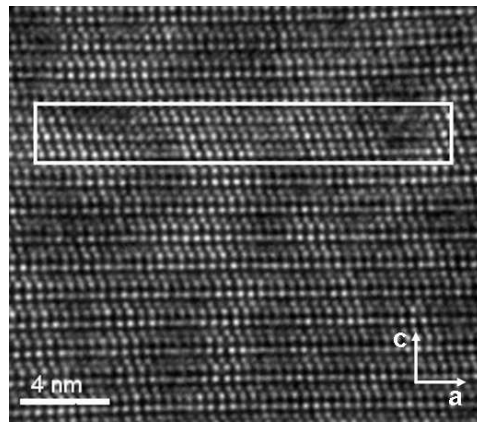


FIG. 1: TEM image in the a - c plane of the $\text{Sr}_3\text{Ru}_2\text{O}_7$ domain as cut from the eutectic. The arrows indicate the area with the atomic stacking of the Sr_2RuO_4 phase.

fects.

The structure and crystalline quality of the samples were assessed by a high resolution triple axis X-ray diffractometer, with a $\text{Cu K}\alpha$ source equipped with a four-circle cradle. The diffraction peaks of sample 1 were identified with the expected $(00l)$ Bragg reflections coming from $\text{Sr}_3\text{Ru}_2\text{O}_7$ and Sr_2RuO_4 , demonstrating both the absence of any spurious phase and the common direction of the c -axes of the two phases. Pole figures proved that also the in-plane axes of the two phases were aligned. It is worth pointing out that XRD spectrum from sample 3 collected with a step size of 0.0002 degrees and time per step of 150 seconds, showed the absence of any Sr_2RuO_4 peak indicating that in the interacting volume, the Sr_2RuO_4 percentage is lower than that one detectable from the surface of the sample.

Hence, by combining the TEM, the X-ray and the EDS/WDS analysis we may conclude that, if present, the size of Sr_2RuO_4 inclusions dispersed in the sample 3, as one, two or three individual layers in a $\text{Sr}_3\text{Ru}_2\text{O}_7$ matrix, is of the order of a few nanometers in the thickness. The upper limit of the volume fraction of these Sr_2RuO_4 layers is 5%. Such percentage can be obtained by combining the systematic TEM analysis[9] and evaluating the difference between the measured average n with respect to that expected for the ideal $\text{Sr}_3\text{Ru}_2\text{O}_7$ stoichiometry.

We have studied the I - V characteristics of the samples 2 and 3 at low temperatures by using a ^3He refrigerator to cool the system down to 0.3 K. All the transport measurements have been performed in Napoli by a standard four-point technique applying the bias current within a - c planes and the magnetic field along c -axis. Contact leads have been placed on the crystals to minimize uncontrollable and complicated pattern of the current flow through the sample. The electrical leads are Al-Si wires, $50 \mu\text{m}$ in diameter, and the contact area is about $100 \times 100 \mu\text{m}^2$. For the transport analysis we used

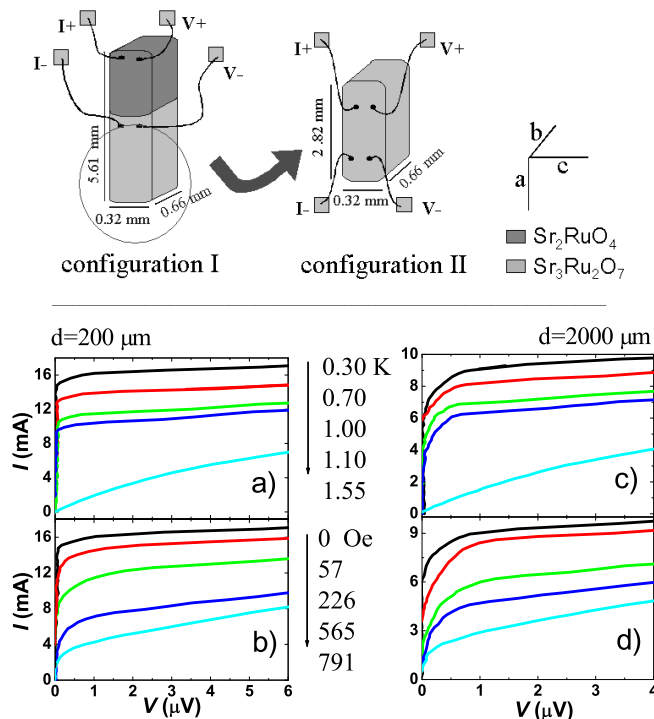


FIG. 2: Top: sketch of electrical leads at different positions on sample 2 (configuration I) and on sample 3 (configuration II), respectively. Bottom: I - V characteristics of sample 2 measured with contact leads in the configuration I at two different distances from the Sr_2RuO_4 - $\text{Sr}_3\text{Ru}_2\text{O}_7$ interface: a) $H = 0$ T and T ranging from 1.5 K to 0.3 K, b) $T = 0.3$ K and $H \parallel c$ -axis ranging from 0 to 750 Oe, $d \simeq 200 \mu\text{m}$; c) $H = 0$ T and T ranging from 1.5 K to 0.3 K, d) $T = 0.3$ K and H ranging from 0 to 750 mT, $d \simeq 2000 \mu\text{m}$.

two different measurement configurations. The configuration I has two contacts in the Sr_2RuO_4 region and the other two in $\text{Sr}_3\text{Ru}_2\text{O}_7$ one at a distance $d \simeq 200 \mu\text{m}$ from the interface (see top side of Fig. 2). In the same configuration, the contacts are placed in the $\text{Sr}_3\text{Ru}_2\text{O}_7$ region at $d \simeq 2000 \mu\text{m}$ away from the interface. In the configuration II the contacts are placed only on the sample 3. All the current and voltage leads were attached using an ultrasound bonder. The measurement of the resistance versus temperature in the configuration I below 2 K yields a SC transition at $T_{c0} = 1.39$ K. We do not observe extra features as measured by a.c. susceptibility on the same eutectic samples[8]. The value found is slightly lower than the SC transition temperature in the best Sr_2RuO_4 pure single crystals ($T_{c0} = 1.5$ K) and nearly the same as that one observed in Ref.[8] within the $\text{Sr}_3\text{Ru}_2\text{O}_7$ region ($T_{c0} = 1.31$ K) cut from the eutectic. This unexpected result is confirmed by I - V characteristics reported in Fig. 2a and Fig. 2b. Below T_{c0} a finite well defined zero-voltage current, I_c , is observed. This behaviour was reproducibly found for all Sr_2RuO_4 - $\text{Sr}_3\text{Ru}_2\text{O}_7$ junctions. The zero-voltage current presents

all the hallmarks of a typical supercurrent: it is increased by decreasing the temperature and is reduced by applying an external magnetic field (see Fig. 2a and Fig. 2b), respectively. By assuming that the whole cross-sectional area was involved in the current path, the critical current density, J_c , is estimated about 7.1 A/cm^2 at 0.3 K and zero applied magnetic field. Remarkably, by placing the contact leads at a distance $d \sim 2000 \mu\text{m}$ far from the interface, a critical current is again observed for temperature below $T_{c0} \sim 1.39$ K (see Fig. 2c). I - V curves measured at different temperatures and magnetic fields show a behaviour similar to the previous one as shown in Fig. 2c and Fig. 2d. In this case, the J_c value is about 3.5 A/cm^2 at 0.3 K. It proves that the supercurrent flows on a long length scale weakly depending on how far the contacts on the $\text{Sr}_3\text{Ru}_2\text{O}_7$ part are from the interface with the Sr_2RuO_4 region.

In order to clarify the role played by the occurrence of an anomalous proximity effect induced by the Sr_2RuO_4 macrodomain connected to the $\text{Sr}_3\text{Ru}_2\text{O}_7$ part, we have performed transport measurements on sample 3 as presented in Fig. 3 (configuration II). From the behaviour of the resistance versus temperature $R(T)$ it is possible to extract again a SC transition at $T_{c0} = 1.39$ K at zero applied magnetic field, showing that a supercurrent is sustained in the $\text{Sr}_3\text{Ru}_2\text{O}_7$ macrodomain independently on the presence of the Sr_2RuO_4 area. In Fig. 3 we present the evolution of the resistance versus temperature at different selected magnetic field. Here, $T_c(H)$ and $H_{c2||c}(0)$ are defined as the temperature and magnetic field for which the resistance reaches 20% of the normal state resistance. Fig. 3 shows the H_{c2} - T phase diagram obtained from the $R(H) - T$ curves. The upper critical field at zero temperature $H_{c2}(T = 0)$ can be estimated by data interpolation with a resulting amplitude for field along the c -axis, $H_{c2||c}(0) \simeq 100$ mT. This value is comparable to that of Sr_2RuO_4 single crystals with $T_c \sim 1.4$ K but substantially different from the value 1 T obtained in the 3-K phase samples[10].

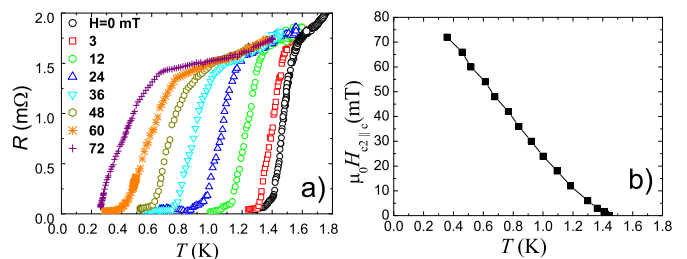


FIG. 3: a) Resistance vs temperature of the sample 3 measured with contact leads in configuration II at different applied field, b) extrapolated upper critical field vs temperature.

One has to address the origin and the nature of the SC features observed in the I - V within the $\text{Sr}_3\text{Ru}_2\text{O}_7$ part of the eutectic. Our considerations start from the basic aspects that, as single crystal phase, the Sr_2RuO_4

is homogeneously SC while the $\text{Sr}_3\text{Ru}_2\text{O}_7$ does not exhibit any SC feature down to very low temperature. Further, the microstructural analysis within the $\text{Sr}_3\text{Ru}_2\text{O}_7$, as cut from the eutectic, reveals a tiny concentration of Sr_2RuO_4 defects either made by stacking faults RuO monolayers, or Sr_2RuO_4 regions clusters. Hence, the observation of a superflow, within the sample 3 and at large distances from the interface in the sample 2, can have three possible scenarios: i) the $\text{Sr}_3\text{Ru}_2\text{O}_7$ is not SC and the supercurrent flows via percolation through the Sr_2RuO_4 defects as in a proximity network, ii) the $\text{Sr}_3\text{Ru}_2\text{O}_7$ has an inhomogeneous superconductivity that supports, together with the Sr_2RuO_4 inclusions, the supercurrent flowing within the entire sample, iii) the $\text{Sr}_3\text{Ru}_2\text{O}_7$ is a homogeneous SC system.

For the case i), it is difficult to account for a flow of supercurrent in the sample 3 as a conventional percolation phenomena through a proximity network made of Sr_2RuO_4 centers separated by normal areas of $\text{Sr}_3\text{Ru}_2\text{O}_7$. The main problem comes from the observed distances between the nodes of the network. Taking into account the de Haas-van Alphen measurements [11] and the theoretical band structure predictions[12], it is possible to obtain the in- and out of plane normal coherence length in the clean limit for the $\text{Sr}_3\text{Ru}_2\text{O}_7$ of the order of $\xi_N^a \simeq 40 T^{-1} \text{K nm}$ and $\xi_N^c \simeq 2.5 T^{-1} \text{K nm}$ ($\xi_N^i = \hbar v_F^i / 2\pi k_B T$, where $i = a, c$ are the axis directions), respectively. Those estimations for the leaking of Cooper pairs in the *normal* $\text{Sr}_3\text{Ru}_2\text{O}_7$ are not compatible both qualitatively and quantitatively with the observed SC features. Hence, the scenario i) can work only if some sort of unconventional mechanism allows for an enhancing of the proximity length within the $\text{Sr}_3\text{Ru}_2\text{O}_7$ domain.

One such possibility is related with the presence of the nanometric Sr_2RuO_4 inclusions that can act as pairs scattering centers for the electrons in the $\text{Sr}_3\text{Ru}_2\text{O}_7$ bands. In this case, areas of RuO monolayers, where pairing without long-range order would occur in the d_{xy} band, act along the c direction as local centers for pair exchange with the electrons in the bands of the $\text{Sr}_3\text{Ru}_2\text{O}_7$ having (d_{xz}, d_{yz}) character. The latter mechanism is favored because of the specific electronic structure and symmetry of the t_{2g} bands[13]. The pairs in the RuO monolayer would behave like effective charge impurity for the electron propagation along the c -axis while the interband scattering allows for pair-exchange between electrons in neighbor layers. It emerges a picture similar to the charge Kondo model[14] and a mechanism for long-range order between pairs in different Sr_2RuO_4 inclusions analog of the RKKY(Ruderman-Kittel-Kasuya-Yosida) interaction between spins. For the charge Kondo model the effective coupling amongst two pair/isospins, mediated by particle-particle excitations, at a distance d is $I(d) = (J^2 \rho_f / 8\pi) / d^3$ where J is the effective local pair exchange and ρ_f is the density of states at the Fermi level. Assuming a concentration x of randomly placed

Sr_2RuO_4 inclusions (resonant pairing centers) the mean-field estimation of the SC percolation temperature gives $T_{c-eut} \cong x J^2 \rho_f \log(D / (x J^2 \rho_f))$ in terms of the bandwidth D [15]. Thus, given for the $\text{Sr}_3\text{Ru}_2\text{O}_7$ the estimated ρ_f (~ 5 states/eV), D (~ 2 meV)[12] and considering that the rate of interlayer pair scattering J is larger than D (J/D ranges in the interval [4–8]) one obtains a value of $T_{c-eut} \sim 1\text{K}$ for a percentage window [2%–8%] of Sr_2RuO_4 inclusions.

The scenario ii) and iii) invokes the possibility that part or the entire $\text{Sr}_3\text{Ru}_2\text{O}_7$ system becomes SC. Such circumstance requires a motivation of the lack of superconductivity in the crystals of $\text{Sr}_3\text{Ru}_2\text{O}_7$ not grown as eutectic. While iii) is unlikely to occur, it might be possible that the small difference in lattice parameters between the Sr_2RuO_4 and the $\text{Sr}_3\text{Ru}_2\text{O}_7$ results in a strain that induces pair formation within the $\text{Sr}_3\text{Ru}_2\text{O}_7$ domain in the form of inhomogeneous patterns. A more detailed microstructural analysis is required to get extra insights in such issues.

In conclusion, we have shown that the $\text{Sr}_3\text{Ru}_2\text{O}_7$, as extracted from the Sr_2RuO_4 - $\text{Sr}_3\text{Ru}_2\text{O}_7$ eutectic system, exhibit unconventional SC features. The SC state seems to be affine with that of Sr_2RuO_4 because there occurs no negative interference in the supercurrent flow at the single interface between Sr_2RuO_4 and $\text{Sr}_3\text{Ru}_2\text{O}_7$ macrodomains. The microstructural analysis gives a clear indication of the amount and size of Sr_2RuO_4 or other spurious phases within the $\text{Sr}_3\text{Ru}_2\text{O}_7$ matrix. Such information excludes a simple percolation via a proximity network to justify the observed supercurrent and points the attention on the role of nanometric RuO stacking faults monolayer in assisting (driving) the pair leaking (formation).

We would like to acknowledge valuable discussions with C. Noce.

-
- [1] Y. Maeno *et al.*, Nature **372**, 532 (1994).
 - [2] A.P. Mackenzie *et al.*, Rev. Mod. Phys. **75**, 657 (2003).
 - [3] S.I. Ikeda *et al.*, J. Phys. Soc. Jpn. **73**, 1322 (2004).
 - [4] S.A. Grigera *et al.*, Science **306**, 1154 (2004).
 - [5] R.A. Borzi *et al.*, Science **315**, 214 (2007).
 - [6] R. Fittipaldi *et al.*, J. Crystal Growth **282**, 152 (2005).
 - [7] J. Hooper *et al.*, Phys. Rev. B **73**, 132510 (2006).
 - [8] S. Kittaka *et al.*, preprint cond-mat/0607151.
 - [9] R. Ciancio *et al.*, unpublished (2007).
 - [10] T. Ando *et al.*, J. Phys. Soc. Jpn. **68**, 1651 (1999).
 - [11] R.A. Borzi *et al.*, Phys. Rev. Lett. **92**, 216403 (2004).
 - [12] D.J. Singh and I.I. Mazin, Phys. Rev. B **63**, 165101 (2001).
 - [13] M.E. Zhitomirsky and T.M. Rice, Phys. Rev. Lett. **87**, 057001 (2001).
 - [14] A. Taraphder and P. Coleman, Phys. Rev. Lett. **66**, 2814 (1991).
 - [15] A.G. Malshukov, Solid State Commun. **77**,57 (1991).